Title

STUDY OF THE REACTION K+ p ->K| n+p AT Gev/c

Authors

Lind, V. Gordon
Alexander, G.
Firestone, A.
et al.

Publication Date

1969-08-05

Submitted to Nuclear Physics B

STUDY OF THE REACTION $K^+p \rightarrow K^0\pi^+p$ AT 9 GeV/c

V. Gordon Lind, G. Alexander, A. Firestone, C. Fu, and G. Goldhaber

August 5, 1969

AEC Contract No. W-7405-eng-48

LAWRENCE RADIATION LABORATORY
UNIVERSITY of CALIFORNIA BERKELEY

DISCLAIMER

UCRL-19284

STUDY OF THE REACTION $K^+p \rightarrow K^o\pi^+p$ AT 9 GeV/c*

V. Gordon Lind,† G. Alexander,‡ A. Firestone, C. Fu, and G. Goldhaber

Department of Physics and Lawrence Radiation Laboratory
University of California, Berkeley, CA 94720

August 5, 1969

ABSTRACT

We present results on the study of the reaction $K^+p \rightarrow K^o\pi^+p$ at 9 GeV/c. The reaction proceeds almost entirely through the production of K^*_{890}, K^*_{1420} and Δ^{++}_{1236}. The spin parity of the K^*_{1420} is shown to be $J^P = 2^+$, with 18% pseudoscalar and 72% vector exchange in its production, the same proportion as for K^*_{890} production. The dependence of the cross sections on incident momentum for the reactions $K^+p \rightarrow K^*_{890}p$, $K^*_{1420}p$, and $K^o\Delta^{++}_{1236}$ appear to fall somewhat more rapidly than the predictions of a simple Regge pole exchange model.

---

*Work supported by the U. S. Atomic Energy Commission.

†Permanent address: Utah State University, Logan, Utah.

‡Permanent address: Tel-Aviv University, Tel-Aviv, Israel.

The reaction $K^+p \rightarrow K^o\pi^+p$ has been studied at numerous momenta ranging from 0.865 to 13.0 GeV/c[1-3]. We report here on the results of a study on a sample of 517 such events at a beam momentum of 9 GeV/c. Only those events within a restricted fiducial volume for which the K^o decays were visible in the bubble chamber were used in the analysis.

The experiment was carried out with ~ 150 000 pictures taken in the 80-inch hydrogen bubble chamber at the Brookhaven National Laboratory Alternating Gradient Synchrotron, exposed to a 9-GeV/c rf-separated K^+ beam. The two-prong-plus-vee events were measured with the LRL Flying Spot Digitizer, and the remeasurements were carried out with a conventional digitizing machine. The events were then spatially reconstructed and kinematically fitted in the program SIOUX to the following hypotheses:

$$K^+p \rightarrow K^o\pi^+p \qquad (1)$$

$$\rightarrow K^o\pi^+\pi^o p \qquad (2)$$

$$\rightarrow K^o\pi^+\pi^+ n \quad . \qquad (3)$$

In addition, various hypotheses, in which the vee decay is either a Λ or $\overline{\Lambda}$ hyperon decay, were attempted. No difficulty was encountered in separating the K^o decays from the Λ or $\overline{\Lambda}$ hyperon decays. The four-constraint production vertex, reaction (1), was preferred to the one-constraint reactions (2) and (3); but ionization consistency was required of all events. The peripheral nature of the interaction allowed complete discrimination between the π^+ and proton tracks for reaction (1) using both kinematic and ionization information. The sample of 517 events of reaction (1) obtained as above are thus essentially unambiguous and without contamination.

The dominant features observed in the reaction are the production of the known K^*_{890}, K^*_{1420}, Δ^{++}_{1236} resonances in addition to a small phase space background.

The Dalitz plot of $M^2(p\pi^+)$ vs $M^2(K^o\pi^+)$ is shown in Fig. 1. We note from this scatter plot that the separation of K^*_{890}, K^*_{1420}, and Δ^{++}_{1236} resonances is particularly clean. This may also be seen in the three mass projections which are shown in Fig. 2. The relative strength of each resonance and the mass and width of each resonance were determined by the maximum likelihood fitting program MURTLEBERT[4]). The program used standard Breit-Wigner line shapes as given by Jackson[5]), corresponding to orbital angular momentum $\ell = 1$ for K^*_{890}, $\ell = 2$ for K^*_{1420}, and $\ell = 1$ for Δ^{++}_{1236}. A flat phase space background over the Dalitz plot, was assumed for this fit. However, since the percentage of phase space background is very small, the detailed shape of the background could not have affected the results of the fit in any significant way. We have treated the mass, width, and relative strength of each of the three resonances as free parameters. We have restricted the accepted events to a fiducial volume and weighted the events to correct for K^o escape probability. The results of this fit are shown in Table 1, and also as the smooth curves shown superimposed on the data in Fig. 2, which represent the data well.

The entire reaction is highly peripheral in nature. This is shown in the angular distributions in Fig. 3. The K^o is produced strongly forward in the production center of mass, the proton strongly backward, and the π^+ either strongly forward or strongly backward depending on whether it makes a Δ^{++}_{1236} with the proton or a K^*_{890} or K^*_{1420} with the K^o.

Scatter plots of the decay angular correlations for the $K^o\pi^+$ mass combination with Δ^{++}_{1236} removed are shown in Fig. 4. Here θ is the angle between the incident K^+ and the K^o in the $K^o\pi^+$ center of mass and φ is the Treiman-Yang angle. The scatter plots show the obvious K^*_{890} and K^*_{1420} resonance bands mentioned earlier. Although the φ distributions show both resonances to have a similar $\sin^2 \varphi$-like distribution, the $\cos\theta$ distributions are obviously different for the two K^* resonances. This may be seen more clearly in the projections in $\cos\theta$ and φ shown in Fig. 5 in the K^*_{890} and K^*_{1420} regions. To account for this difference in the $\cos\theta$ distributions either the exchange mechanisms for the production of the two resonances are different or else they have different spins and parity, or both. The spin-parity of the K^*_{890} is well known to be $J^P = 1^-$ and that of the K^*_{1420} is favored to be $J^P = 2^+$; however, 1^- is not excluded. We have used the maximum likelihood method to fit the data in the K^*_{1420} region to the angular distributions expected for $J^P = 1^-$ and $J^P = 2^+$ particles. The expected distributions, assuming only pseudoscalar and vector exchange, are given by[5]):

$$W_1(\theta,\varphi) = \frac{3}{4\pi}\{\rho_{00} \cos^2\theta + \rho_{11} \sin^2\theta - \rho_{1,-1} \sin^2\theta \cos 2\varphi - \sqrt{2}\, \mathrm{Re}\, \rho_{10} \sin 2\theta \cos\varphi\}$$

$$W_2(\theta,\varphi) = \frac{15}{16\pi}(3\, \rho_{00}[\cos^2\theta - \tfrac{1}{3}]^2 + 4 \sin^2\theta \cos^2\theta[\rho_{11} - \rho_{1,-1} \cos 2\varphi])$$

for $J^P = 1^-$ and $J^P = 2^+$ respectively.

The ρ_{ij} coefficients are those corresponding to the spin density matrix elements, and for the above assumption have the additional trace and positivity conditions:

$$2\, \rho_{11} = 1 - \rho_{00}$$

$$|\rho_{1,-1}| \leq \rho_{11} \quad .$$

In the maximum likelihood fit the best values for the ρ_{ij} matrix elements were determined. The predicted angular distributions were then compared with the actual data by looking at the $\cos\theta$ and φ projections (see Fig. 5). The smooth curves correspond to the best fit predictions. The assumption of $J^P = 1^-$ for the K^*_{890} is observed to give an excellent fit to the data and the values for the ρ_{ij} thus determined are given in Table 2. For the K^*_{1420} the best fits are given by the dashed and solid lines on Fig. 5c and d, which represent the $J^P = 1^-$ and $J^P = 2^+$ distributions respectively. It is noted that the $J^P = 1^-$ fit is very poor whereas $J^P = 2^+$ fits well. In addition, the $J^P = 1^-$ fit requires 100% pseudoscalar exchange, which is in strong disagreement with the φ distribution as shown in Fig. 5d. We thus conclude the spin-parity of the K^*_{1420} is $J^P = 2^+$, although we have not attempted to fit the data to still higher spin values. Here it should be noted that the $J^P = 2^+$ fit for the K^*_{1420} requires the same exchange mechanism as the $J^P = 1^-$ fit for K^*_{890}; i.e., 18% pseudoscalar and 72% vector exchange. We did not consider it necessary to make background corrections due to the cleanness of the data, and in addition we felt that attempts to make background corrections may even be hazardous due to our lack of understanding of the processes in the mass region between the two K^* resonances.

We point out one additional feature in the decay correlations of the $K^o\pi^+$ system (see Fig. 3). That is, at a $(K^o\pi^+)$ mass of about 1160 and over a region of about 100 MeV in width, a distinct distribution in the cos θ plot may be seen which appears to differ from those in the other regions. The distribution in θ in this region looks like $\sin^2\theta \cos^2\theta$, whereas the distribution in φ in the same mass region is consistent with being flat, although from the available data no reliable shape can be determined. A small enhancement at this region is also observed in the projected $K^o\pi^+$ mass plot (Fig. 2a). This effect could be due to an additional K^* resonance at a mass of about 1160 mentioned by other investigators[6].

A best fit for the decay correlations of the Δ^{++}_{1236} were also obtained. The values for the spin density matrix elements ρ_{ij} are given in Table 2 and the agreement between the fit and the data is shown in Figs. 5e and f. The spin density matrix elements we report for the K^*_{890} and Δ^{++}_{1236} are, in general, in reasonable agreement (always less than 2 standard deviations away) with those reported by the CERN-Bruxelles[1]), Birmingham-Glasgow-Oxford[2]) and Rochester[3]) groups and with our own data at 4.6 GeV/c[7]). The values obtained for Δ^{++}_{1236} are in general good agreement with those predicted by the Sakurai-Stodolsky model[8]). (See Table 2.)

A study of $d\sigma/dt$ where t is the square of the four-momentum transfer to the proton for the K^*_{890}, K^*_{1420}, and Δ^{++}_{1236} bands gives good fits to distributions of the form Ae^{Bt}. The data and best fits are shown in Fig. 6. We have plotted the data as a function of t, rather than t' where $t' = t - t_{min}$, and t_{min} is the minimum value of t allowed by kinematics for the appropriate value of $M(K\pi)$ or $M(p\pi)$, because at this incident momentum the difference in distributions is negligible. The CERN-Bruxelles collaboration[1]) report a forward dip for $-t' < 0.2$ $(GeV/c)^2$ in both the K^*_{890} and Δ^{++}_{1236} distributions at 5 and 8.25 GeV/c. The British collaboration[2]) report a forward dip at $-t < 0.1$ $(GeV/c)^2$ for the K^*_{890} at 10 GeV/c, and the Rochester group[3]) reports similar results at 12.7 GeV/c. We observe a flattening of the K^*_{890} distribution for $-t < 0.1$, but present statistics do not permit a statement about a dip in the forward direction. We note, however, in agreement with the CERN-Bruxelles result, that the cross sections do not approach zero as $t' \to 0$.

In Fig. 7 we show the variation of the cross sections with momentum for the reactions $K^+p \to K^o\pi^+p$, $K^o\Delta^{++}_{1236}$, $K^*_{890}p$, and $K^*_{1420}p$ for incident momenta from 3 to 13 GeV/c. The data are from the CERN-Bruxelles collaboration[1]), the British collaboration[2]), the Rochester group[3]) and our own data at 4.6 GeV/c (Ref. 7) and 9 GeV/c. We have plotted $\ln \sigma$ vs $\ln p$ for each of the reactions and have performed a least squares fit to the data for a function of the form $\sigma = Kp^{-n}$ suggested by Morrison[9]), where p is the incident momentum and K is some constant. The values of n thus obtained are shown in Table 3, together with the predictions of a simple Regge model, based on ω exchange for the $K^*_{890}p$ state, ρ and ω exchange for the $K^*_{1420}p$ state and ρ and A_2 exchange for the $K^o\Delta^{++}_{1236}$ state. The simple Regge exchange model has the principal energy dependence of the cross section in the form $s^{2(\alpha(t)-1)}$ which we approximate by $s^{2(\alpha(0.1)-1)}$, since the bulk of the cross section for these reactions occurs at low values of $|t|$; specifically, the average value of $|t|$ is about 0.1 $(\mathrm{GeV/c})^2$. We note that at high incident momentum s is proportional to p. In general the dependence of the cross section on energy is somewhat greater than that predicted by this simple expression, as has been noted previously[1,2,9]).

In conclusion, our data show clearly a peripheral production of K^*_{890}, K^*_{1420}, and Δ^{++}_{1236} and suggest the presence of an additional resonance K^*_{1160}. The decay correlations show the spin parity of the K^*_{1420} to be $J^P = 2^+$, with 18% pseudoscalar and 72% vector exchange taking place in the production. The possibility of a 1^- assignment for the K^*_{1420} is clearly inconsistent with the data. The K^*_{890} is also produced with an 18% pseudoscalar and 72% vector exchange mechanism, which is the same proportion as that for the production of K^*_{1420}. The dependence of the cross sections on incident momentum for the reactions $K^+p \rightarrow K^*_{890}p$, $K^*_{1420}p$, and $K^o\Delta^{++}_{1236}$ appear inconsistent with the predictions of a simple Regge pole exchange model.

We wish to thank R. D. Mathews for helpful discussions. We also thank R. Shutt and the staff of the 80-inch bubble chamber and H. Foelsche and the AGS staff at Brookhaven for helping with the exposure. We acknowledge the valuable support given by H. White and the FSD staff and by our programing and scanning staff, in particular D. V. Armstrong and E. R. Burns. One of us, G. Lind, wishes to further express appreciation to the Lawrence Radiation Laboratory, and in particular to the Trilling-Goldhaber Group, for their hospitality during the three months spent at the Laboratory.

Table 1

Reaction cross sections and fitted parameters

Reaction	σ (μb)	Percent	Mass (MeV)	Width (MeV)
$K^+p \to K^o\pi^+p$	275±41	100		
$K^+p \to K^o\Delta^{++}_{1236}$	107±23	39±2	1207±4	82±9
$K^+p \to K^*_{890}p$	97±23	35±2	895±2	50±7
$K^+p \to K^*_{1420}p$	36±14	13±2	1414±11	107±19

Table 2

Spin density matrix elements

Resonance	Matrix elements		(Stodolsky-Sakurai)
Δ^{++}_{1236}	$\rho_{3,3}$	0.32±0.05	0.38
	Re $\rho_{3,-1}$	0.16±0.05	0.22
	Re $\rho_{3,1}$	-0.07±0.04	0
K^*_{890}	$\rho_{0,0}$	0.19±0.05	
	$\rho_{1,1}$	0.41±0.03	
	$\rho_{1,-1}$	0.44±0.03	
	Re $\rho_{1,0}$	-0.02±0.02	
K^*_{1420}			
$J^P = 2^+$	$\rho_{0,0}$	0.18±0.08	
	$\rho_{1,1}$	0.39±0.04	
	$\rho_{1,-1}$	0.40±0.05	
$J^P = 1^-$	$\rho_{0,0}$	1.02±0.13	
	$\rho_{1,1}$	-0.01±0.06	
	$\rho_{1,-1}$	0.10±0.06	
	Re $\rho_{1,0}$	0.05±0.04	

Table 3

Fits to $\sigma = Kp^{-n}$

		Regge model	
Final state	n (experimental)	Exchanges	n (predicted)
$K^*_{890}p$	1.9±0.1	ω	1.4
$K^*_{1420}p$	1.7±0.2	ω,ρ	1.4
$K^o\Delta^{++}_{1236}$	2.1±0.1	ρ,A_2	1.4

REFERENCES

1) W. De Baere, J. Debaisieux, P. Dufour, F. Grard, J. Heughebaert, L. Pape, P. Peeters, F. Verbeure, R. Windmolders, G. Bassompierre, D. Drijard, Y. Goldschmidt-Clermont, A. Grant, V. P. Henri, B. Jongejans, D. Lingliu, F. Muller, J. M. Perreau, H. Piotrowska, I. Saitov, R. Sekulin, and G. Wolf, K^* and N^* production in the $K^o p \pi^+$ final state at K^+ incoming momenta from 3 to 8.25 GeV/c, paper submitted to the XIVth International Conference on High-Energy Physics, Vienna, 1968.

2) Birmingham-Glasgow-Oxford Collaboration, Two-Body Final States Produced in K^+-Proton Interactions at 10 GeV/c, Proceedings of the Topical Conference on High-Energy Collisions of Hadrons, Vol. II, CERN 68-7, p. 121.

3) J. C. Berlinghieri, M. S. Farber, T. Ferbel, B. E. Forman, A. C. Melissinos, P. F. Slattery, and H. Yuta, Nucl. Phys. B8 (1968) 333.

4) MURTLEBERT, Alvarez Programing Group Note P-156, J. H. Friedman, Lawrence Radiation Laboratory, Berkeley, 1966 (unpublished).

5) J. D. Jackson, Nuovo Cimento 34 (1964) 1644.

6) D. J. Crennell, U. Karshon, K. W. Lai, J. S. O'Neall, and J. M. Scarr, Phys. Rev. Letters 22 (1969) 487.

7) C. Fu, Study of the Reaction $K^+p \rightarrow K^o\pi^+p$ at 4.6 GeV/c and a Review of the Available Data, Lawrence Radiation Laboratory Report UCRL-18417, 1968 (unpublished).

8) L. Stodolsky and J. J. Sakurai, Phys. Rev. Letters 11 (1963) 90; L. Stodolsky, Phys. Rev. 134 (1964) B1099.

9) D. R. O. Morrison, Phys. Letters 22 (1967) 528.

FIGURE CAPTIONS

Fig. 1. Dalitz plot of $M^2(p\pi^+)$ vs $M^2(K^o\pi^+)$.

Fig. 2. (a) $M(K^o\pi^+)$; (b) $M(p\pi^+)$; (c) $M(K^op)$. The smooth curves are the results of the fit to the Dalitz plot distribution.

Fig. 3. Center-of-mass production angles. (a) K^o vs p; (b) π^+ vs K^o.

Fig. 4. Scatter plots of $M(K^o\pi^+)$ vs (a) $\cos\theta$, where θ is the angle between the incident K^+ and the K^o in the $K^o\pi^+$ center of mass; (b) φ (Treiman-Yang angle).

Fig. 5. Decay angular distributions. (a) K^*_{890}, $\cos\theta$; (b) K^*_{890}, φ; (c) K^*_{1420}, $\cos\theta$; (d) K^*_{1420}, φ; (e) Δ^{++}_{1238}, $\cos\theta$; (f) Δ^{++}_{1238}, φ.

Fig. 6. Distributions in $-t$ for (a) Δ^{++}_{1238}; (b) K^*_{890}; (c) K^*_{1420}.

Fig. 7. Cross sections as a function of incident momentum for the reactions $K^+p \to$ (a) $K^o\pi^+p$, (b) $K^o\Delta^{++}_{1236}$, (c) $K^*_{890}p$, and (d) $K^*_{1420}p$.

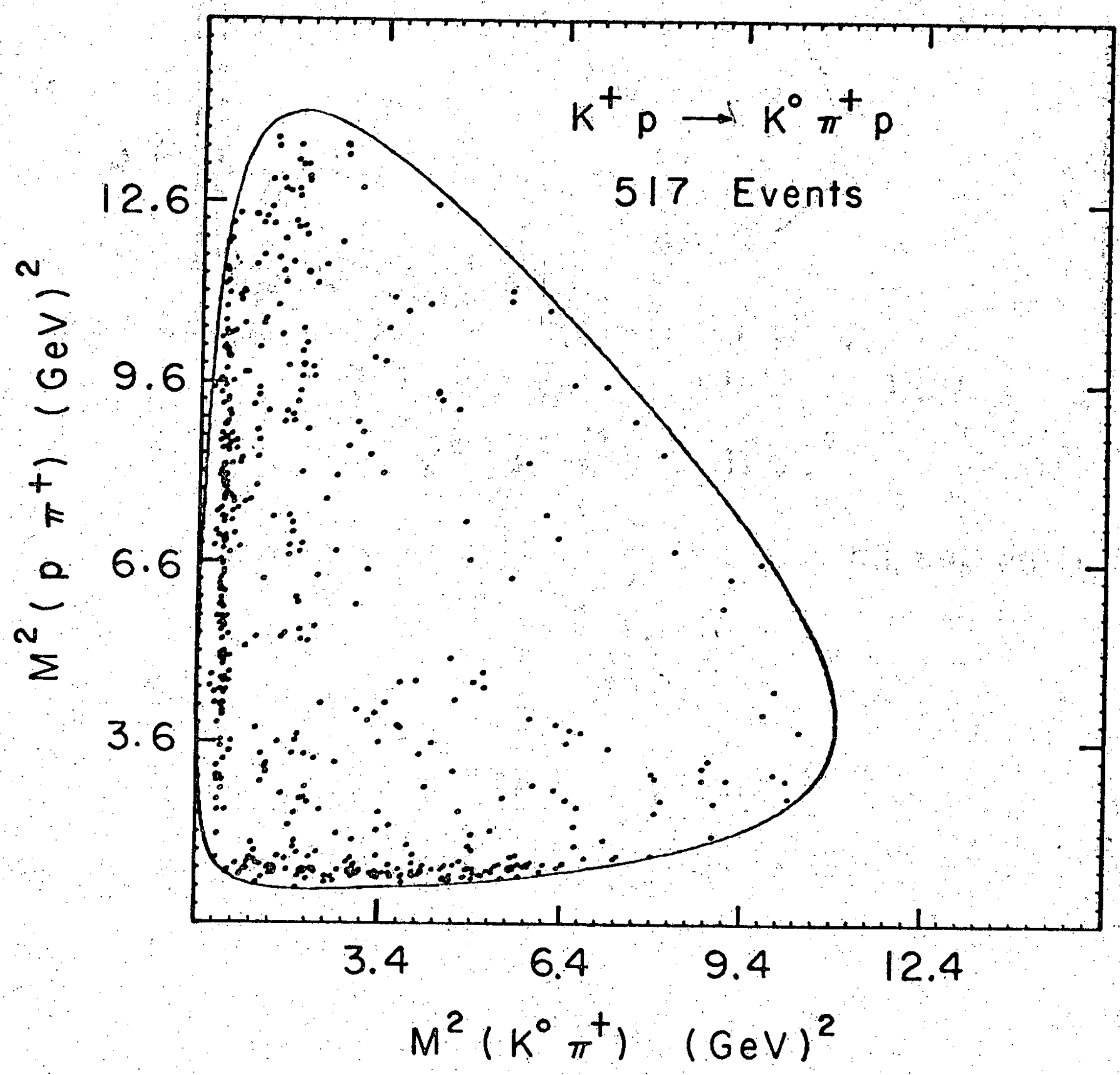

XBL695-2840

Fig. 1

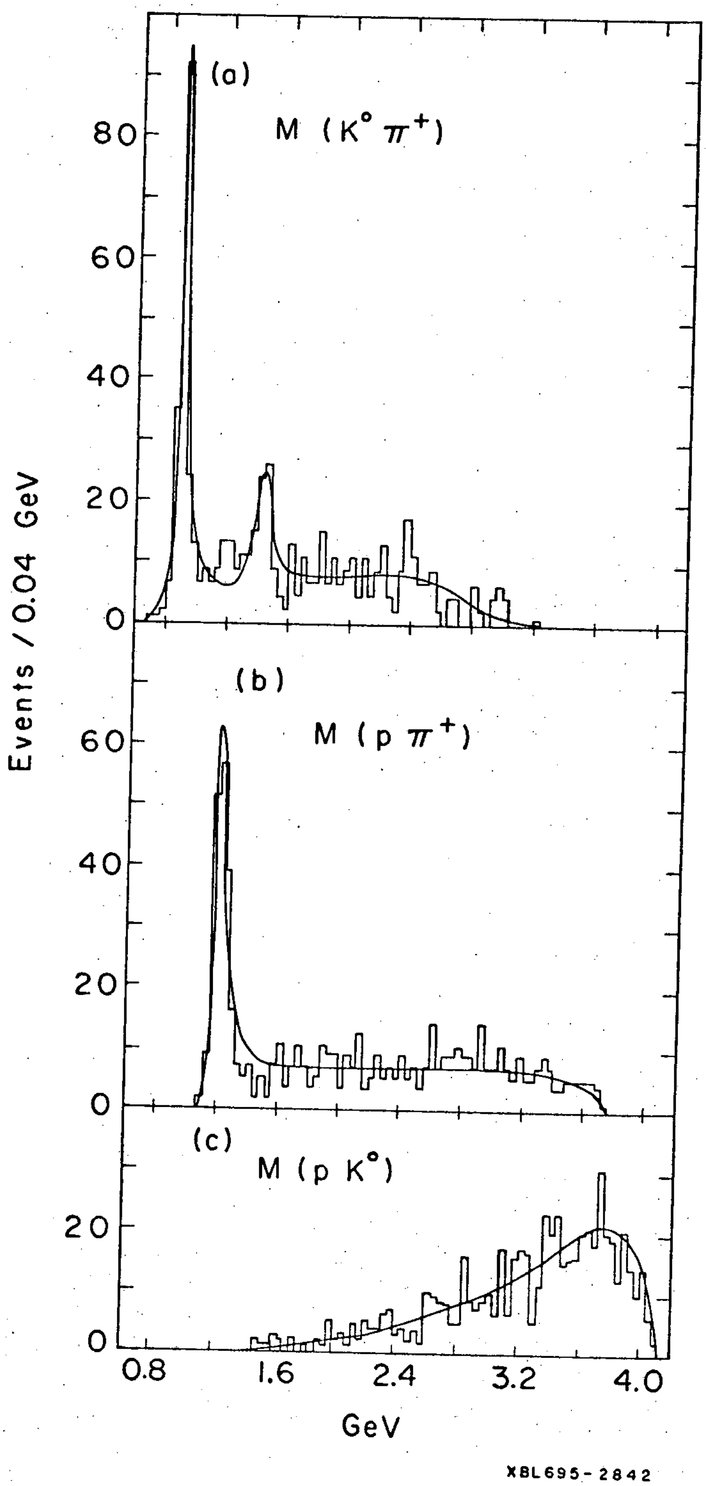
(a)
M (K° π⁺)
80
60
40
20
0
Events / 0.04 GeV
(b)
M (p π⁺)
60
40
20
0
(c)
M (p K°)
20
0
0.8
1.6
2.4
3.2
4.0
GeV
XBL695-2842

Fig. 2

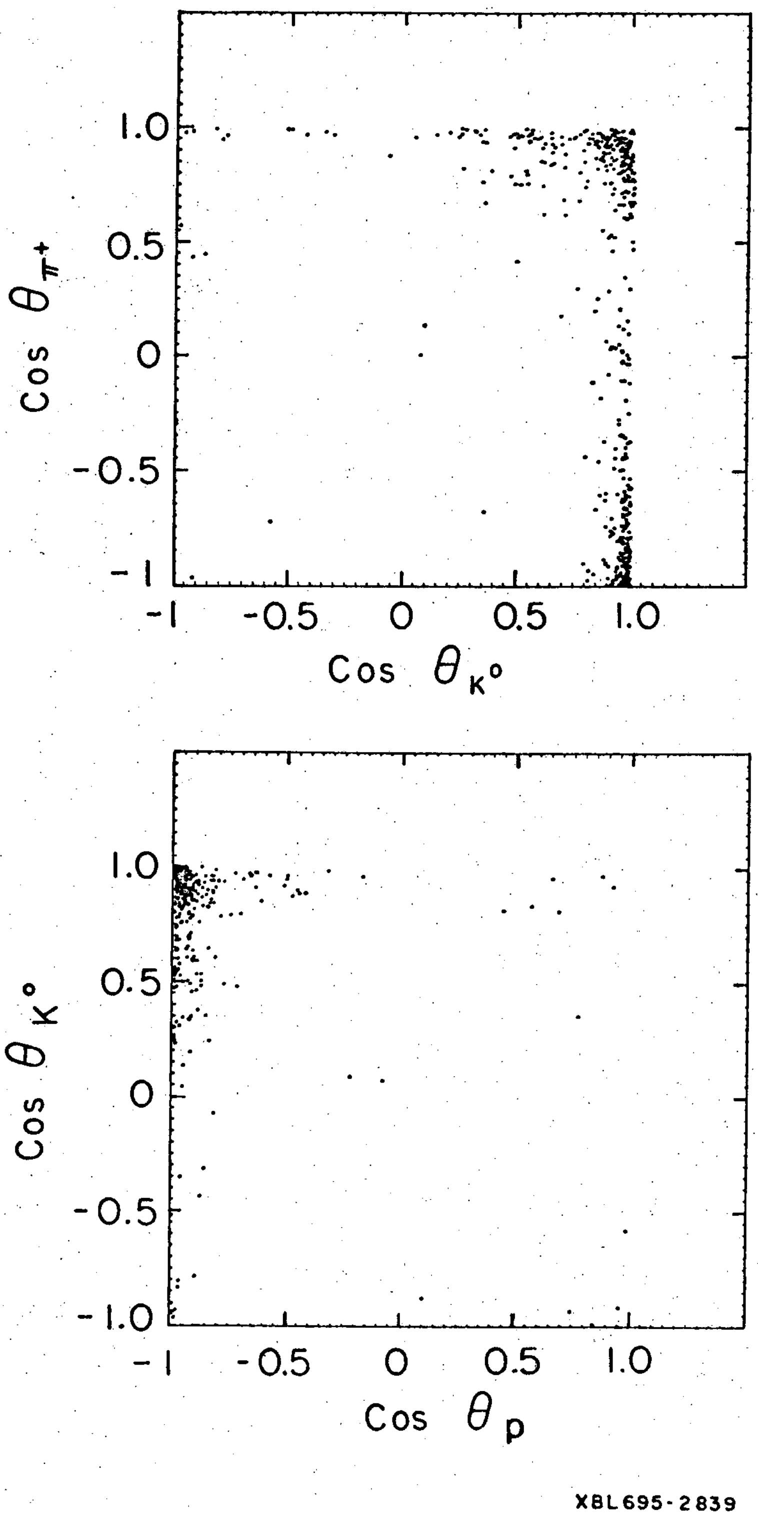
1.0
0.5
0
-0.5
-1
Cos θ π+
-1
-0.5
0
0.5
1.0
Cos θ K°
1.0
0.5
0
-0.5
-1.0
Cos θ K°
-1
-0.5
0
0.5
1.0
Cos θ p
XBL695-2839

Fig. 3

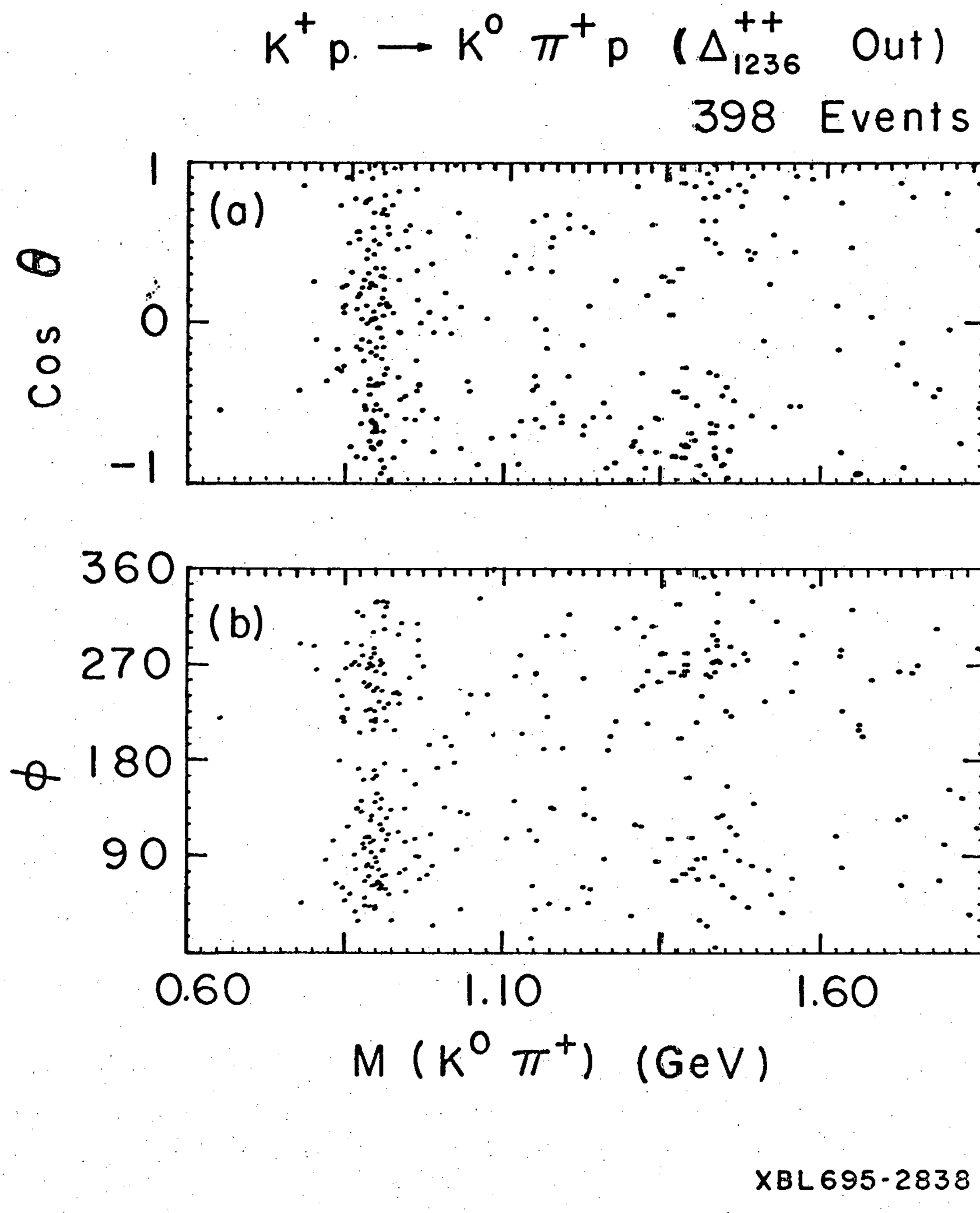
$K^+p \longrightarrow K^0 \pi^+ p$ (Δ^{++}_{1236} Out)
398 Events
(a)
Cos θ
1
0
−1
(b)
φ
360
270
180
90
0.60
1.10
1.60
M ($K^0 \pi^+$) (GeV)
XBL695-2838

Fig. 4

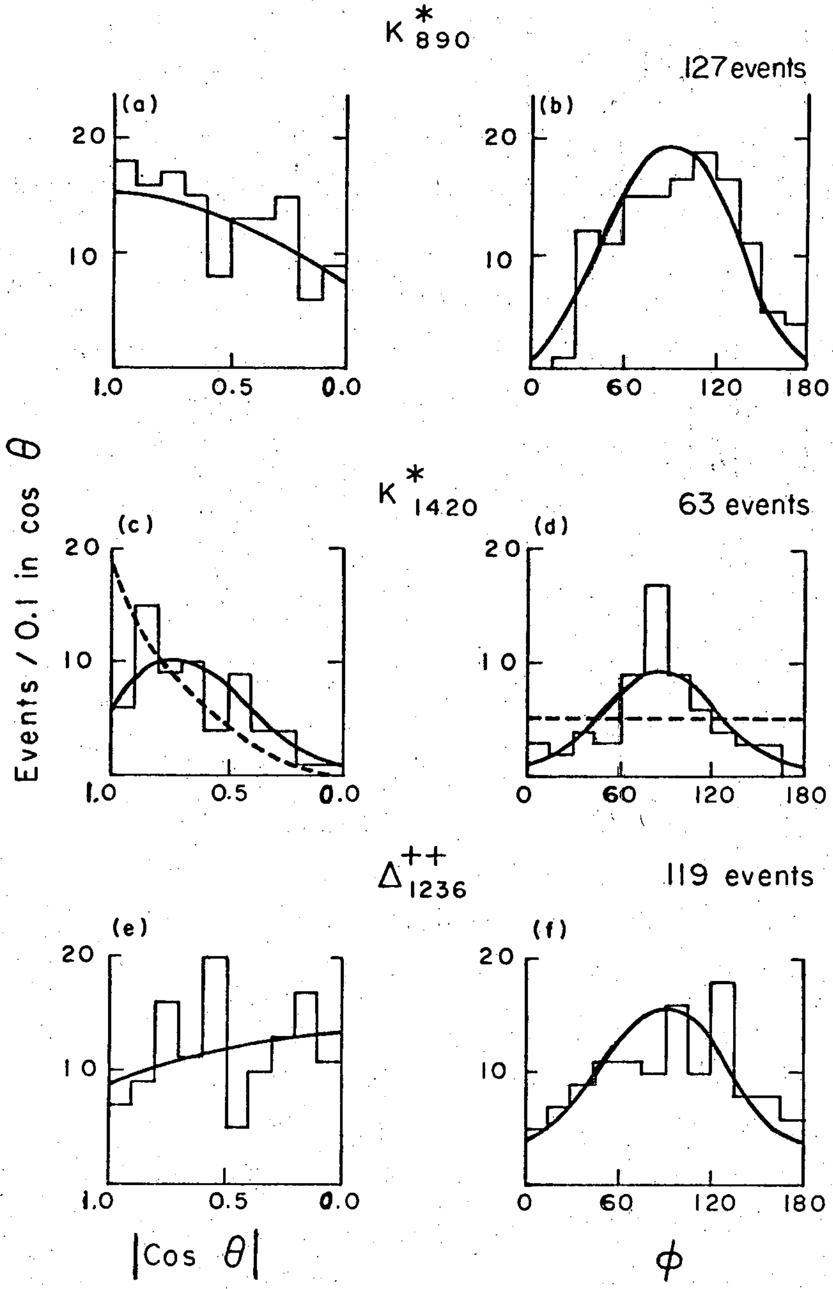

XBL695-2836

Fig. 5

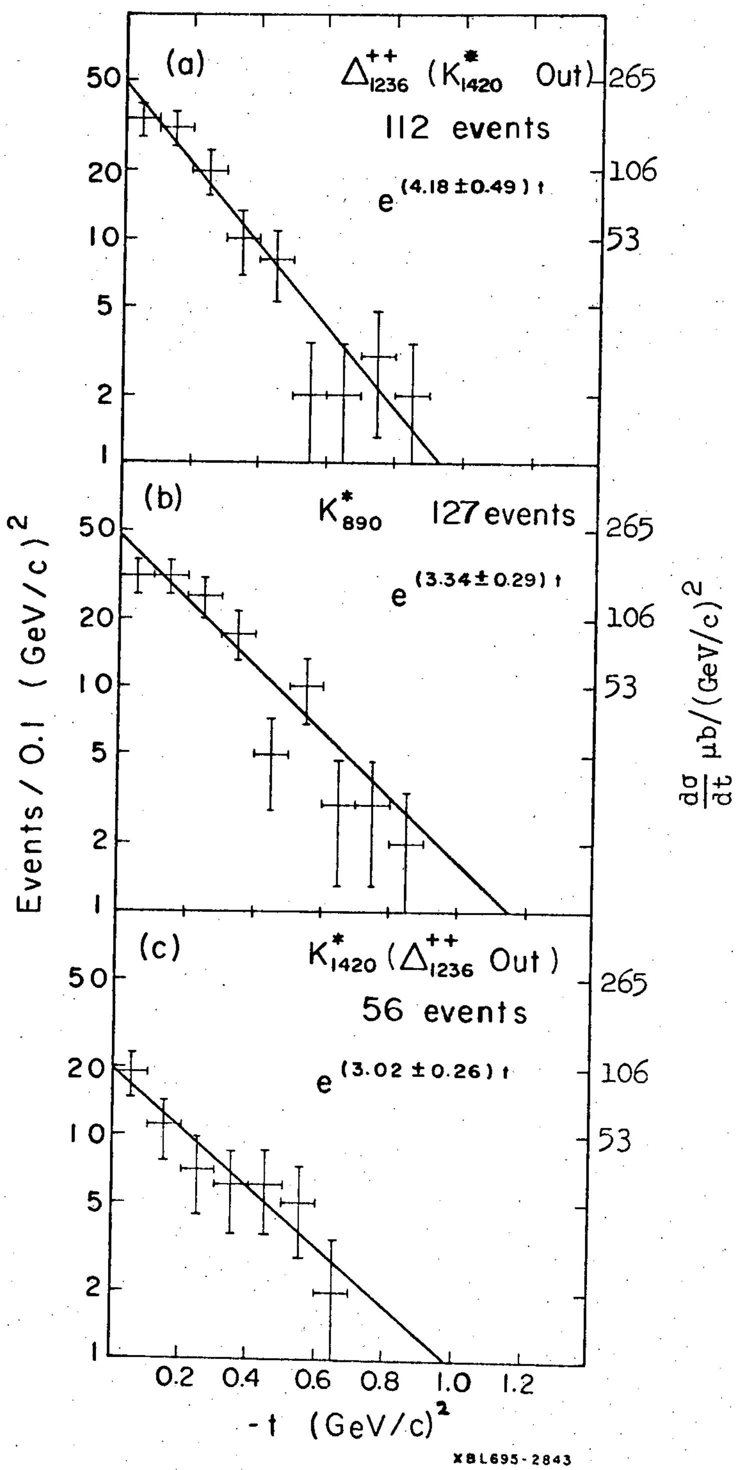
(a)
Δ^{++}_{1236} (K^*_{1420} Out)
112 events
$e^{(4.18\pm0.49)t}$
(b)
K^*_{890} 127 events
$e^{(3.34\pm0.29)t}$
(c)
K^*_{1420} (Δ^{++}_{1236} Out)
56 events
$e^{(3.02\pm0.26)t}$
Events / 0.1 $(GeV/c)^2$
$\frac{d\sigma}{dt}$ $\mu b/(GeV/c)^2$
50
20
10
5
2
1
265
106
53
0.2
0.4
0.6
0.8
1.0
1.2
$-t$ $(GeV/c)^2$
XBL695-2843

Fig. 6

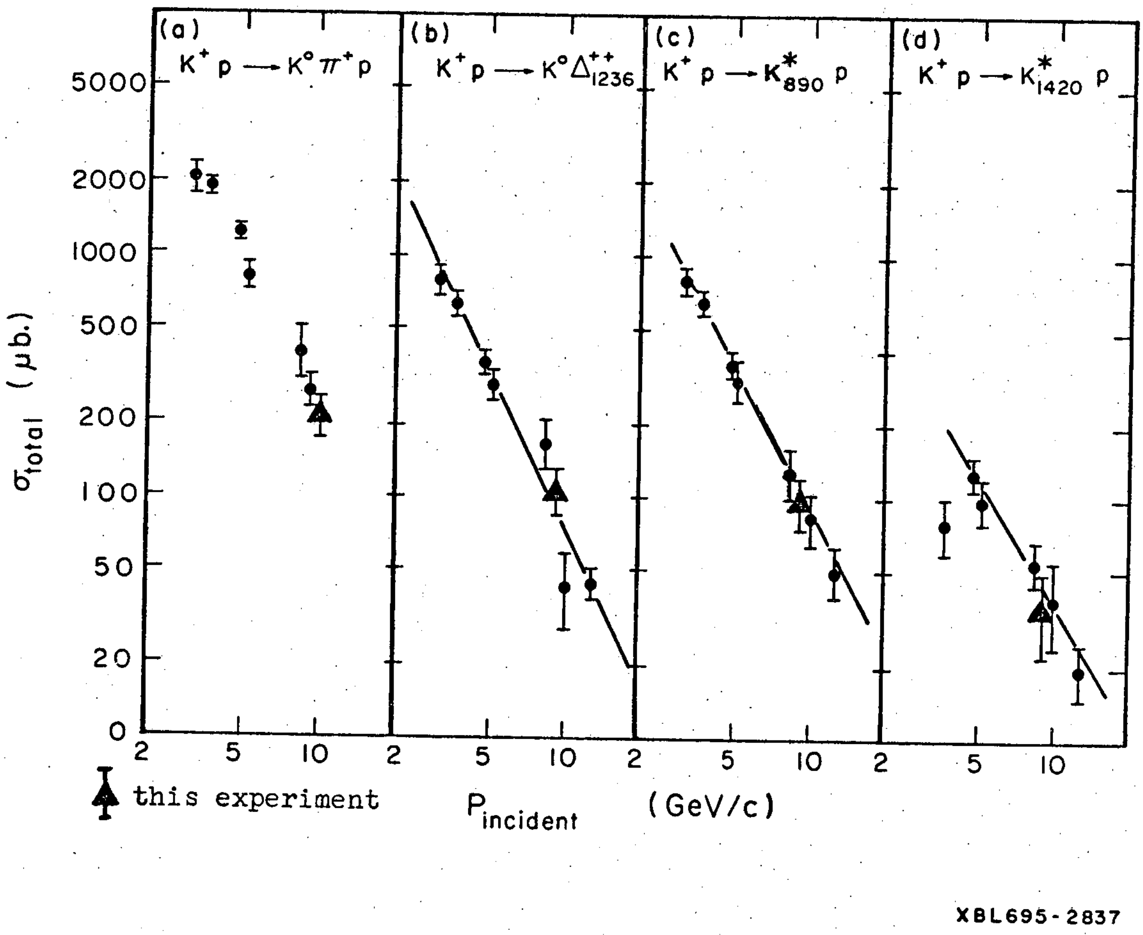
(a)
K⁺ p ⟶ K° π⁺ p
(b)
K⁺ p ⟶ K° Δ⁺⁺ 1236
(c)
K⁺ p ⟶ K* 890 p
(d)
K⁺ p ⟶ K* 1420 p
5000
2000
1000
500
200
100
50
20
0
σ total (μb.)
2
5
10
this experiment
P incident (GeV/c)
XBL695-2837

Fig. 7

TECHNICAL INFORMATION DIVISION
LAWRENCE RADIATION LABORATORY
UNIVERSITY OF CALIFORNIA
BERKELEY, CALIFORNIA 94720